WILEY

Detection of acidic paper recovery after alkaline nanoparticle treatment by 2D NMR relaxometry

G. Poggi[1] 🔵 | A. Parmentier[2] 🔵 | S. Nourinaeini[3] 🔵 | F. De Luca[3]

[1]Department of Chemistry and CSGI, University of Florence, Sesto Fiorentino (Florence), Italy

[2]INFN, Division of Rome Tor Vergata, Rome, Italy

[3]Department of Physics, Sapienza University of Rome, Rome, Italy

Correspondence
Alexandra Parmentier, INFN, Division of Rome Tor Vergata, via della Ricerca Scientifica 1, Rome 00133, Italy.
Email: alexandra.parmentier@roma2.infn.it

Abstract

Cellulose-based artefacts are highly prone to degradation, especially in the presence of acidic compounds, which trigger the depolymerization of cellulose chains and lead to a loss in the original mechanical resistance of the material. Calcium hydroxide nanoparticles dispersed in organic solvent have been recently proposed for the deacidification of cellulose-based artworks. In this work, changes induced on paper by a deacidification treatment, following an acidification bath, were studied by nuclear magnetic resonance (NMR) relaxometry and by the so-called NMR diffraction of water trapped in the cellulose network. The deacidification treatment modifies intrachain and interchain bonds in hydrolyzed and degraded cellulose, leading to a buffered cellulose network configuration, which is similar to that characterizing the untreated reference sample in terms of relaxation parameters. Overall, calcium hydroxide nanoparticles are demonstrated effective in hindering the degradation of cellulose induced by acids and ageing in strong environmental conditions, even from the standpoint of cellulose network arrangement. It is worth noting, too, that the unilateral NMR device used for the relaxation measurements may represent a powerful tool for the preservation of cellulose-based artworks because it allows for the monitoring of the conservation status of cellulose in a completely non-invasive manner.

KEYWORDS

calcium hydroxide nanoparticles, cellulose, deacidification, hydrolysis, NMR relaxometry

1 | INTRODUCTION

A large part of Cultural Heritage assets all over the world consists of cellulose-based materials because cellulose has been widely used since ancient times, in the form of paper, carton, wood, or textile, to write or to create art, thus becoming a ubiquitous medium.

Cellulose is a linear polymer built on cellobiose repeating unit, which consists of two D-glucose molecules linked through a β-1,4-glycosidic bond. The degree of polymerization (DP) of cellulose, which typically ranges from 9,000 to 15,000,[1] is one of the key indices to assess the condition of cellulose-based materials. Hydrogen bonds between hydroxyl groups either of the same chain (intramolecular bonds) or different chains (intermolecular bonds) give raise to the so-called supramolecular structure of cellulose, which is a hierarchical structure that is responsible for several properties of paper, wood, and textiles, including their mechanical features. Single polymeric chains are aggregated to form elementary fibrils, having a transverse extension of a few nanometres; these fibrils are bound together in microfibrils, which usually contain tens of elementary fibrils.[2] On the other hand, macrofibrils, or fibre structures,

having a transverse dimension of tens of micrometres, are obtained by aggregation of microfibrils.[3]

Regions with different chain packing, that is, crystalline and amorphous, are found in elementary fibrils.[1,2] Crystalline regions display highly ordered structures, making them impenetrable to water and highly resistant to degradation. On the other hand, only little or no chain order is found in the amorphous domains (ADs). AD regions behave as hydrophilic sites where water, or other chemical agents, are more free to interact with single cellulose chains[4]; ADs are, therefore, more prone to degradation.[5,6]

Water in cellulose is organized in two phases, which are characterized by different confining environments: one phase is characterized by mobile water (phase-1) and is assigned to ADs located in elementary fibrils at, or close to, fibre surfaces; the other, characterized by less mobile water (phase-2), is confined in microfibril ADs located at fibre cores.[3,7–10] This model agrees with the widespread phenomenological characterization of water in cellulose structures.

The most important degradation mechanism of cellulose is the acid-catalyzed hydrolysis of the β-1,4-glycosidic bonds of chains, resulting in the decrease of cellulose DP and, macroscopically, in the dramatic decay of the mechanical resistance of cellulose-based materials.[11–13] The acidification decay is a recurring event for cellulose-based artefacts because several materials involved in the manufacturing process of these objects are acidic or may develop acidic substances upon ageing. Scientists and conservators have recently paid increasing attention to the conspicuous number of documentary, historical, and artistic cellulosic materials in need of urgent maintenance.[14–18] Therefore, Cultural Heritage cellulose-based materials call for the development of effective conservation strategies to inhibit acid-catalyzed hydrolysis. In recent years, solutions based on nanomaterials and soft matter physics have been introduced in the field of Cultural Heritage conservation.[19,20] These innovative systems are often more efficient, and more compatible with original artefacts, than traditional methods, and they have a broad applicability.

Because of the detrimental impact of acidic substances in the degradation of cellulosic materials, deacidification, that is, the neutralization of acidity, is a key step for the preservation of these Heritage materials.[21,22] One of the most innovative methods for deacidification is based on alkaline nanoparticles dispersed in poorly polar, or nonpolar, solvents. Due to their high surface-to-volume ratio, nanoparticles display a high reactivity towards acids and allow for a fast conversion of hydroxide excess into carbonate. Alkaline nanoparticles, mainly calcium and magnesium hydroxide, have been tested on

waterlogged wood,[23–25] wood from organ pipes,[26] and paper and canvas,[27–33] and they have undergone extensive assessment with very positive results.[34–37] pH and DP measurements and colorimetric and thermal analyses have been used to evaluate the effect of this method for the protection of cellulose-based artworks from acidic degradation, even upon ageing under strong conditions.

New insight into the changes in the macromolecular network of cellulose after acid-catalyzed hydrolysis has been recently obtained using nuclear magnetic resonance (NMR) diffusometry.[9,10] In this work, we have used NMR relaxation and diffraction measurements to monitor the changes in acidic paper due to the application of a deacidification based on calcium hydroxide nanoparticles. Those changes were also monitored during a 2-week ageing at high temperature and relative humidity used to favour the depolymerization of cellulose in untreated, acidic, and deacidified paper. The untreated sample plays the role of the reference standard. Acidification and artificial ageing trigger various processes that influence intrachain and interchain interactions,[38,39] possibly inducing changes in the arrangement of cellulose and therefore on water relaxation characteristics. As a result, the study of relaxation modifications using NMR may provide critical information to establish whether alkaline nanoparticles work as an effective tool in hampering cellulose degradation also from the standpoint of cellulose network arrangement.

2 | MATERIALS AND METHODS

2.1 | Sample preparation

All samples were prepared using commercial Whatman filter paper (Grade 5, 125-mm diameter), which is composed of raw cotton fibres (minimum α-cellulose content: 98%). Acidic paper samples were prepared by immersion in an H_2SO_4 solution (pH = 2.5) for 240 s. Prior to measurements, samples were left under ambient conditions for 2 weeks. These samples are labelled as A.

Untreated filter paper was used as a reference. Because capillarity and pore size can be altered by immersion in water,[4] the reference was immersed in distilled water for 240 s to take into account the effects of mere soaking.[10] Reference samples are labelled as R.

For the preparation of deacidified samples (labelled as D), the following procedure was used: filter paper disks underwent the same acidification process as A samples; after 2 weeks, each disc was treated with 3 ml of calcium hydroxide nanoparticles dispersion in ethanol (1.5 g/L), obtained via a solvothermal process.[31,32] The nanoparticle dispersion was applied on both sides using a

micropipette so as to pour the liquid and homogeneously wet the surface. Samples were then left under ambient condition for 2 weeks.

To trigger the degradation of cellulose, R, A, and D samples were artificially aged under strong hydrothermal conditions. The samples were put in a sealed vessel (5 L), which was placed in an oven at 80°C. Inside the sealed vessel, humidity was kept at 75% using an NaCl saturated aqueous solution. Samples were aged for 2 weeks. Upon removal from the ageing vessel, the samples were labelled as follows: 1-week aged samples as R1, A1, and D1; and 2-week aged samples as R2, A2, and D2.

2.2 | Sample characterization

2.2.1 | pH and DP measurements

pH measurements were performed as follows: 125 mg of sample was weighed, cut into small pieces (about 9 mm^2), and placed inside screw-top vials. 9 ml of distilled water was added to each vial, which was immediately sealed to avoid the solubilization of CO_2 from air into the extracting water. Vials were then kept under stirring for 1 hour before measuring the pH of the extraction using a digital pH-metre (CrisonBasic 20, equipped with a combined electrode, model 52-21). Three measurements were performed on each sample. The associated error is ±0.2.

The DP of cellulose in samples was obtained by viscosimetric measurements.[40] Data are presented in terms of scissions per initial cellulose chain (S^*), calculated by means of the following equation[41,42]:

$$S^* = \frac{DP_{V_0}}{DP_{V_t}} - 1,$$ (1)

where DP_{V_0} is the DP at time zero and DP_{V_t} is the DP at any time t. It is worth noting that an accurate calculation of the number of scissions cannot be extracted from DP_V due to polydispersity, which cannot be assessed by viscosimetric measurements. Nevertheless, in the present work, the comparison of S^* values calculated from DP_V can be considered fully acceptable because the experimental data refer to homologous series of samples. The error associated to these measurements is ±25.

PH and DP_V values were monitored before, during, and after the ageing and are reported in Table 1.

2.3 | Relaxation measurements

Spin-lattice (T1) and spin-spin (T2) correlation relaxometry were performed using a Bruker single-sided mq-ProFiler that works at a static magnetic field of about 0.4 T.[43] The sensitive volume facing the probe surface, where the resonance condition is established, is about $2.0 \times 0.2 \times 0.8$ cm^3. A radiofrequency pulse sequence [saturation $- t_1 - \pi/2 - t_E/2 - (\pi - t_E/2 -$ acquisition $- t_E/2)_n - t_R]_m$ with a recycle time $t_R = 2$ s, an echo time $t_E = 44$ μs, and a number of echoes $n = 500$ was used.[44] The echo time $t_E = 44$ μs prevents the detection of ^1H nuclei different from those belonging to water. The saturation time (t_1) varies in m-step geometric progression from 0.1 ms to 4 s, with an incremental factor 1.3 and 1,024 scans per each value.

The pulse sequence allows obtaining an ($n \times m$) matrix that returns the magnetization distribution

$$M(t_1, t_E) = M_0 \int\int P(\text{T1,T2})k_1(t_1,\text{T1})k_2(t_E,\text{T2})d\text{T1}d\text{T2},$$

(2)

where M_0 is the total equilibrium magnetization, $k_{1,2}$ the relaxation kernels, and $P(\text{T1,T2})$ the correlation map. $P(\text{T1,T2})$ is obtained by an inverse Laplace transform of $M(t_1, t_E)$.[45] Notice that because of pore space heterogeneity, the relaxation-time distributions have in general an asymmetric shape. Therefore, the calculation of mean values of relaxation times is not trivial because any time, which is proportional to pore volume/surface ratio, must be weighted by the corresponding spin population, which is proportional to the cube of volume/surface. A good compromise is the use of the geometric-mean relaxation time, which can be evaluated as a logarithmic mean over the range of time values, weighted by the corresponding spin population.[46] All measurements were performed on samples at room temperature $T = (25 \pm 1)°C$.

TABLE 1 DP_V, S^*, pH, the average spin-spin relaxation time (T2), and confining size for water (d) are summarized for all analysed paper samples

Sample	DP_V	S^*	pH	T2 (ms)	d (μm)
R	920	-	6.7	3.2 ± 0.2	2.5 ± 0.2
R1	683	0.35	6.9	3.0 ± 0.1	2.2 ± 0.1
R2	555	0.66	6.9	2.8 ± 0.1	2.0 ± 0.1
A	551	0.67	4.8	5.2 ± 0.3	3.0 ± 0.2
A1	349	1.64	5.4	3.0 ± 0.1	2.2 ± 0.2
A2	345	1.67	5.3	1.4 ± 0.1	1.9 ± 0.1
D	537	0.71	9.7	3.1 ± 0.1	2.3 ± 0.1
D1	496	0.85	9.2	3.0 ± 0.1	2.2 ± 0.2
D2	504	0.82	8.9	2.8 ± 0.1	2.0 ± 0.2

2.4 | Diffraction measurements

Diffraction measurements were performed using a Brucker Avance 300-MHz spectrometer equipped with a gradient unit that generates a maximum gradient intensity of about 1,200 G/cm. The implemented sequence was the PFG-STE,[47] in which two G gradients of δ duration ($\delta \cong 1.4$ ms) are applied between three 90° pulses. The first two pulses are separated by a time interval $\tau \cong 2.0$ ms, and the second pulse has a delay Δ from the third. For each of the 20 gradient steps, during which the gradient intensity was increased from 0 to 1,050 G/cm, 32 scans were performed. The relaxation recycle delay was fixed at 3 s.

The dynamic wave vector $\vec{q} = \gamma \delta \vec{G}$ and Δ evolution of PFG-STE signal for free water are given by

$$E(q,\Delta) = E(0,\Delta)\exp\left[-q^2 D(\Delta - \delta/3)\right], \qquad (3)$$

where D is the molecular self-diffusion coefficient. In case of restricted diffusion regime, $E(q, \Delta)$ changes, according to the confinement size, in relation to Δ, G, and D.[48]

Prior to tests, paper samples were cut into strips of about 2.5×20 mm^2; after being sealed in a plastic film,

six of these strips were inserted into the NMR tube for measurements.

3 | RESULTS AND DISCUSSION

T1 and T2 correlation maps of the reference samples are reported in Figure 1. In these maps, as well as in the following ones, P(T1,T2) distribution is represented by 10 level curves. The dash-dotted line corresponds to T1 = T2, which characterizes pure bulk water. It is worth noting that the spots on the left side of this line do not have any physical significance. On the right side of the dash-dotted line, several spots can be found. In each map, the upper spot can be associated to the more mobile water located in the ADs of elementary fibrils at, or close, to fibre surfaces. On the contrary, the lower one is related to water trapped in ADs at core fibres.[10,49] This spot is neither affected by the hydration degree of paper nor by ageing and deacidification procedures; for this reason, it will be not further discussed.

As reported in Table 1, water with higher mobility in the unaged reference system (R) is characterized by an average spin-spin relaxation time T2 = 3.2 ± 0.2 ms.
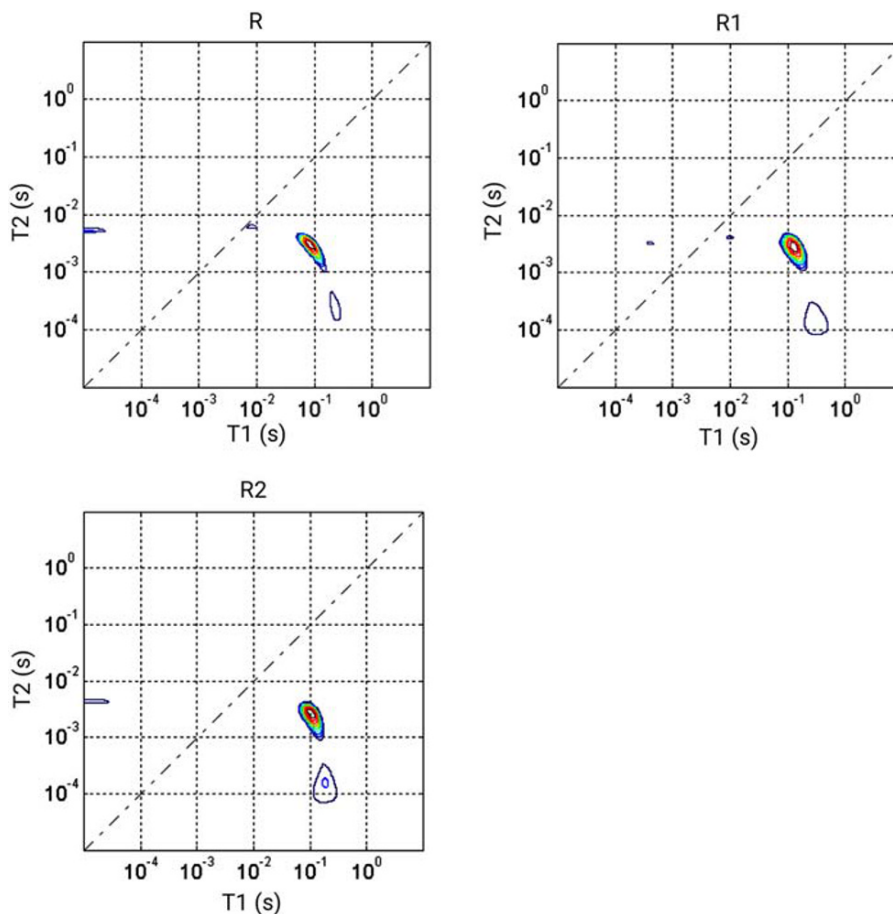

FIGURE 1 Relaxation maps of the reference samples (R, R1, and R2)

Because water mobility is strictly related to its confining sizes, support information about confining dimensions can be obtained by NMR diffraction measurements.[48] NMR diffraction measurements have been therefore performed to relate pore size to water mobility, and hence to T2 relaxation. However, due to heterogeneous cellulose texture, diffraction conditions are more complex than in homogeneous pores. Consequently, only the smallest q dip, which corresponds to largest confining structure, is detectable with some certainty.[48] These largest confining structures of phase-1, which are related to the extension of ADs at, or close to fibers surfaces, approximately establish the upper limit for water mobility. To discern effective diffraction dips from noise, a statistical criterion was used, which allows for assessing the statistically significant q with respect to error distribution.[50]

Yet one has to keep in mind that, in strongly heterogeneous environments investigated by NMR diffraction, diffraction dips often turn out not sharply resolved. Dip selection is based on previous studies on fluid diffusion in porous media,[50] with some caveats deriving from neglecting transverse relaxation processes that contribute to signal attenuation. It is also worth noting that, once again due to heterogeneity, the mean spacing between any two sites corresponds to a generic coherence length embodied by the wavelength associated to wave vector q, which is the actual length to be evaluated in order to retrieve d (with associated errors propagated mainly from Δq, as well as uncertainties on gradient intensity and pulse length). However, the purpose of such measurements is only qualitative, being the relative variation between pore dimensions the more significant aspect.

Diffraction results for the reference samples are reported in Figure 2. In each figure, an arrow marks any statistically significant dip. The confining size for the unaged reference sample (R) is $d = 2.5 \pm 0.1$ μm, as reported in Table 1.

The relaxation map of the 1-week aged reference sample under strong conditions (R1) shows a spot structure very similar to that of the R sample. The upper spot has an average spin-spin relaxation time value $T2 = 3.0 \pm 0.1$ ms, very close to the one of the R sample. This suggests that, after 1 week of artificial ageing, the reference system was poorly modified in terms of the confining size of water, even though some depolymerization occurred, as reported in Table 1. This is confirmed by the diffraction pattern of R1 reported in Figure 2, which returns $d = 2.2 \pm 0.1$ μm. The slight increase of the average T1 value for R1 may suggest a change in the dynamic spectrum of water, even though this conjecture cannot be directly assessed at fixed temperature and fixed NMR frequency. For this reason, T1 shift, which is of
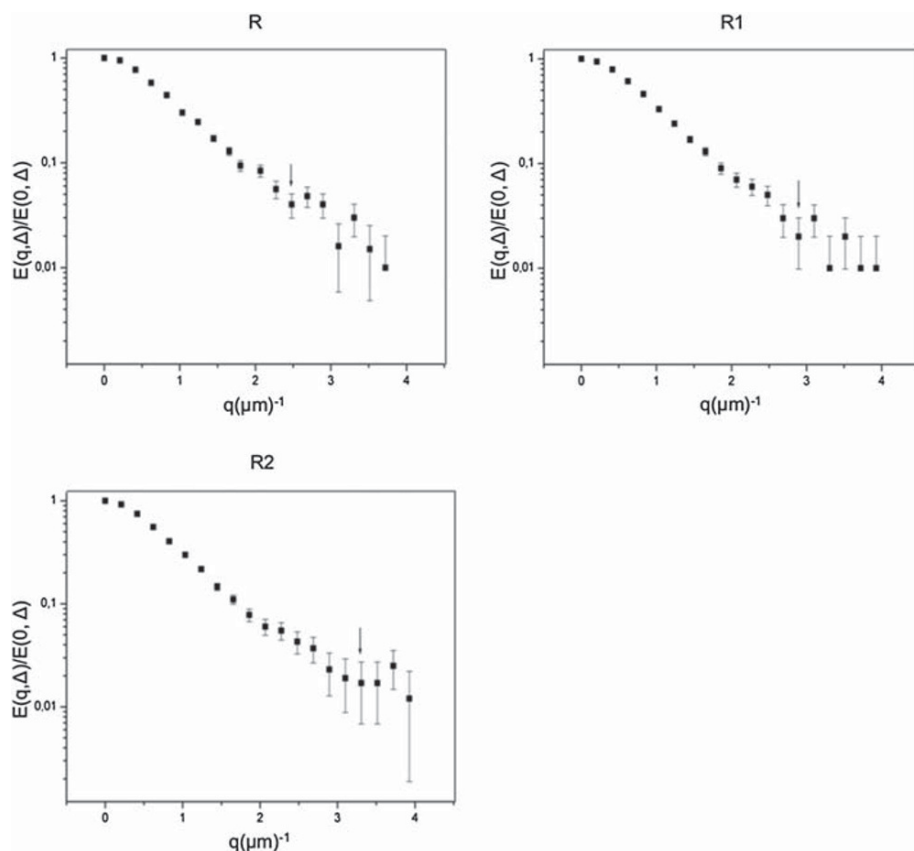

FIGURE 2 Nuclear magnetic resonance diffraction patterns of samples R, R1, and R2. Any arrow marks the first statistically significant dip

negligible entity in all maps, is not reported in Table 1 and will not be further discussed.

The relaxation map of the 2-week aged reference system (R2) shows an average relaxation time T2 = 2.8 ± 0.1 ms, that is, a slightly more appreciable reduction in the relaxation time with respect to the R sample. This can be associated to a further, though small, decrease in the confining size of water. The strong environmental conditions of the artificial ageing are known to trigger the cleavage of cellulose chains at random sites (see S^* values in Table 1) and, at the same time, to favour their mobility due to crosslinking or to the formation of irreversible intrafibre hydrogen bonding, any of which does not affect the DP.[38,39,51] All these phenomena, in particular the latter two, might allow for a more compact arrangement of the fragmented cellulose molecules, resulting in a reduction of the confining size for water and, in turn, of water mobility. This scenario is confirmed by water's confining size in R2 as highlighted by the diffraction dip reported in Figure 2, which returns $d = 2.0 \pm 0.1$ μm. Further support can be found in NMR diffusometry data, reported elsewhere.[52]

The relaxation maps of acidified samples are reported in Figure 3. The acidification bath used for the preparation of these samples (see Materials and Methods section) induced significant decrease in cellulose DP (see Table 1) without triggering crosslinking if compared with R samples' artificial ageing at high temperature and relative humidity. In the acidic samples, we detected an increase in the confining size for water, and a modification of water mobility in the ADs, induced by changes in the conformation and density of the structure due to the detrimental effect of acids on cellulose.[6,42,53] Indeed, A sample has an average spin-spin relaxation time value of T2 = 5.2 ± 0.3 ms, significantly larger than that of R sample. This means that hydrolysis results in the opening of the structure, with a significant increase in pore size of ADs located in elementary fibrils at fibre surfaces, which are accessible to acids, as already shown elsewhere.[9,10] It is also worth noting that the increase in the confining size of water can also allow for the penetration of pollutants inside paper, which may result in new degradation mechanisms, or enhance the acidification process itself.[54–56] The diffraction patterns of the acidified samples are
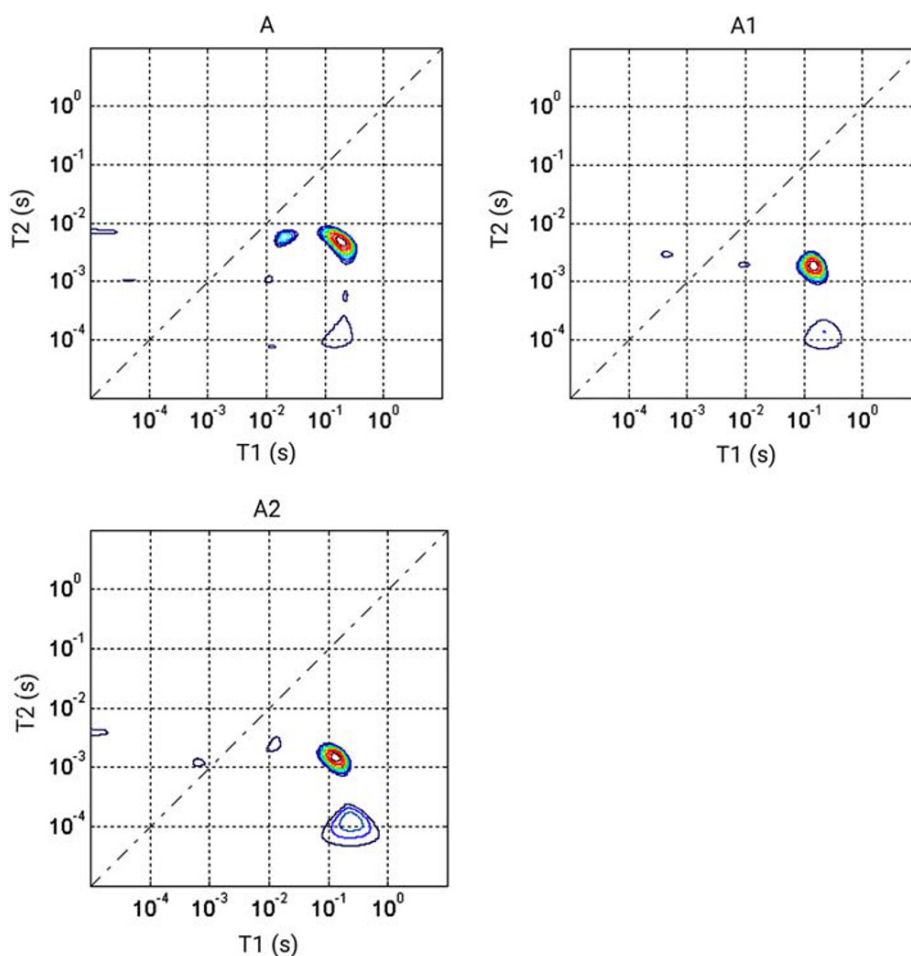

FIGURE 3 Relaxation maps of the acidified samples (A, A1, and A2)

reported in Figure 4. Diffraction data concerning A sample confirm the increase of the confining size for water up to a dimension of $d = 3.0 \pm 0.2$ μm.

The map of the 1-week aged acidic sample (A1) shows an average relaxation time $T2 = 3.0 \pm 0.1$ ms, whereas the A2 sample, artificially aged for 2 weeks, exhibits an average relaxation time $T2 = 1.4 \pm 0.1$ ms. The confining sizes are $d = 2.2 \pm 0.2$ μm and $d = 1.9 \pm 0.1$ μm, respectively. As mentioned above, the hydrothermal treatment of paper induces the depolymerization of cellulose at random sites and triggers the mobility of cellulose chains, thus favouring a rearrangement in the fragmented cellulose molecules by crosslinking and intrafibre hydrogen bonding.[38,39,51] It is interesting to note that, in the case of acidic samples, the reduction of the average T2 values is drastic, which probably means that, in such samples, the formation of intramolecular and intermolecular bonds during ageing increases remarkably, especially after the first week. Indeed, as clearly shown in Table 1, DP values of A1 and A2 are almost equal, confirming that in samples A2, crosslinking is favoured with respect to depolymerization. This is probably due to average chain length of cellulose being close to the so-called levelling off DP corresponding to the DP of crystallites, which cannot be further depolymerized.[6,57]

The different behaviour of acidic and reference samples is remarked by their respective T2 values. Specifically, the relative T2 variation of R1 with respect to R is about 6%, whereas that of R2 with respect to R is about 12%. On the contrary, the relative T2 variation of A1 with respect to A is about 38% and that of A2 with respect to A is about 73%. The final effect of ageing causes A1 sample to have the same confining size of R1, whereas that of the A2 sample is reduced with respect to R2; this is fully confirmed by diffusion data reported elsewhere.[52] This means that water mobility is similar in A1 and R1 samples, whereas it is reduced in A2 with respect to R2 sample. These conclusions are fully supported by confining sizes obtained by diffraction dips (Figure 4), even though they scale with different relative amplitudes, as T2 monitors the confining size by means of the local magnetic field.[58]

It has been already demonstrated that alkaline nanoparticles have a fundamental role in hampering the depolymerization of cellulose because of the neutralization of acidity.[23–25,27–33] The maps of deacidified samples are reported in Figure 5. Interestingly, alkaline nanoparticles modify the texture of cellulose chains in the ADs. In particular, the neutralization of sulfuric acid here allows for a rearrangement of the smaller fragment of cellulose fibers. This rearrangement can be also
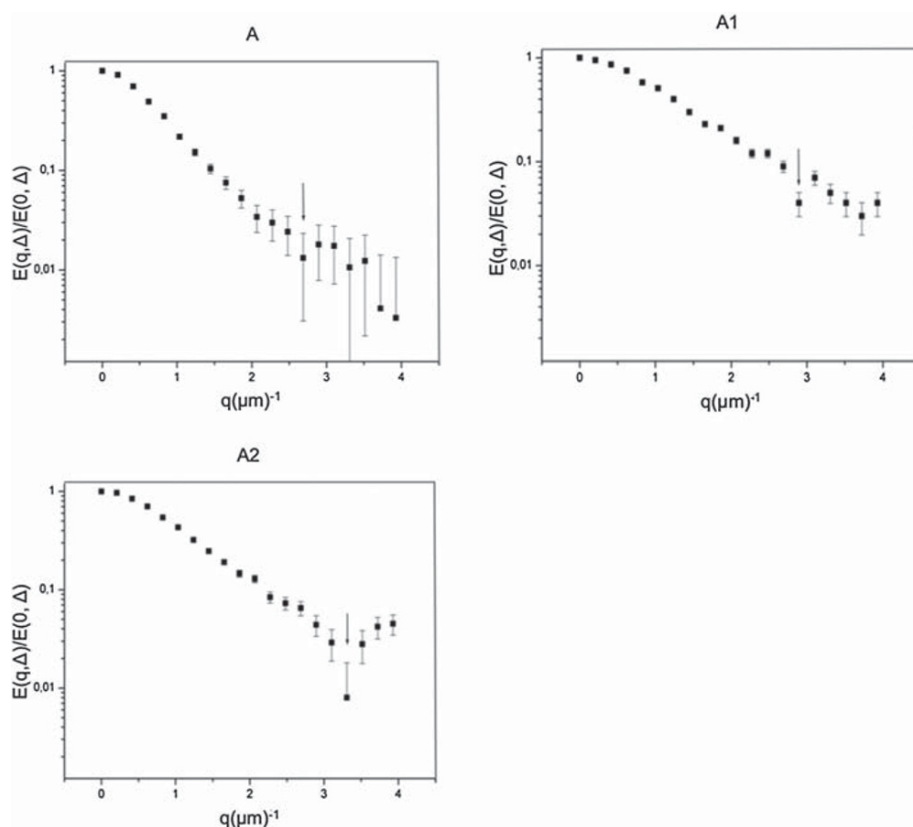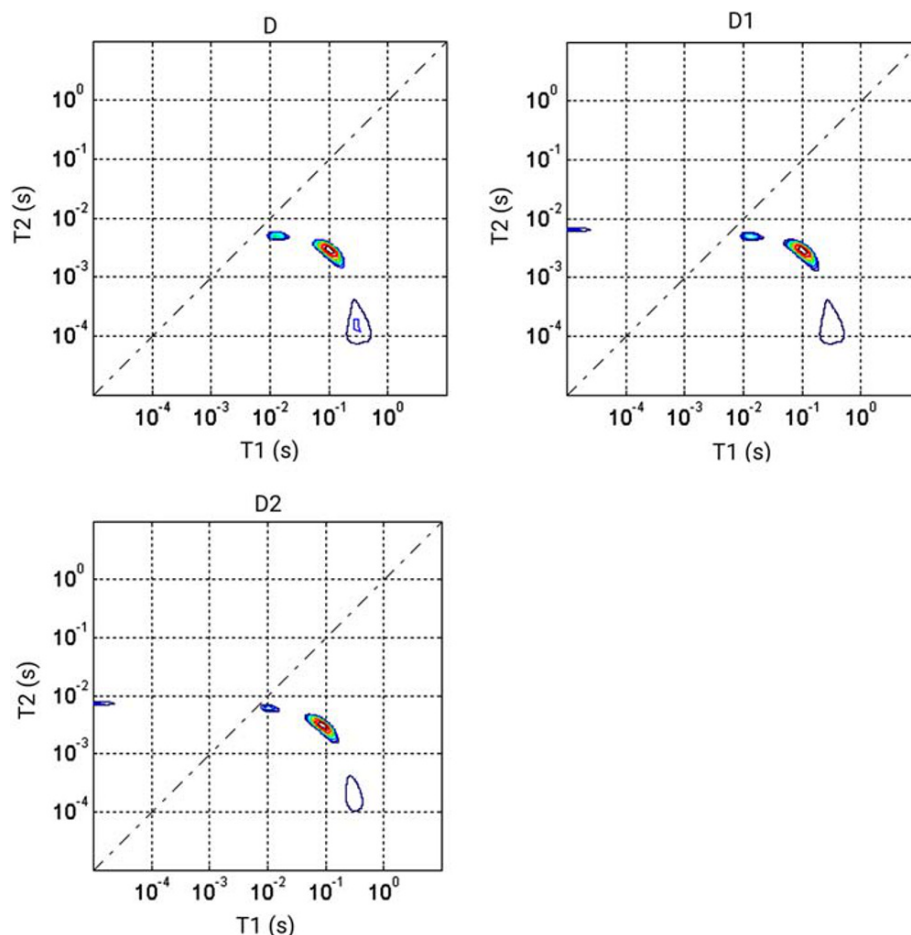

FIGURE 4 Nuclear magnetic resonance diffraction patterns of samples A, A1, and A2. Any arrow marks first statistically significant dip

FIGURE 5 Relaxation maps of the deacidified samples (D, D1, and D2)

ascribed to the fact that divalent calcium ions of alkaline nanoparticles can interact with carboxylate groups from different cellulose chains or belonging to the same chain,[31,59,60] thus resulting in a more tightly packed network.

The rearrangement in the D sample induces a conformation of the cellulose network that is similar to that of the reference system R, in spite of the fact that, as expected, the DP of D sample, before the artificial ageing, is the same as the one characterizing the acidic sample A (see Table 1). In fact, depolymerization is an irreversible process, and glycosidic bonds cannot be restored after cellulose degradation. Nonetheless, the benefits of a neutralization process carried out by alkaline nanoparticles are remarked by cellulose arrangement. Indeed, the average spin-spin relaxation time of D sample is $T2 = 3.1 \pm 0.1$ ms, close to that characterizing the reference sample.

Upon artificial ageing, the presence of alkaline nanoparticles hampers the depolymerization of cellulose, as shown by the S^* values of D1 and D2, which are lower than those of A1 and A2, respectively, by a factor 2. Correspondingly, the average spin-spin relaxation time of D1 sample is $T2 = 3.0 \pm 0.1$ ms and that of D2 sample is

$T2 = 2.8 \pm 0.1$ ms. Both these values are very similar to those characterizing R1 and R2, respectively, which suggests that, in reference and deacidified samples, confining sizes for water are comparable. Diffraction patterns of deacidified samples are reported in Figure 6. Such data return the following confining sizes: $d = 2.3 \pm 0.1$ μm for the D sample, $d = 2.2 \pm 0.2$ μm for the D1 sample, and $d = 2.0 \pm 0.2$ μm for the D2 sample, in full consistence with the scenario lined by relaxation data and further supported by diffusion measurements reported elsewhere.[52]

Overall, in deacidified samples, the unilateral NMR measurements show a restructuring of cellulose texture in ADs even after an acidification bath and a subsequent ageing under strong conditions. This recovery can be associated to the action of alkaline nanoparticles used for the deacidification treatment, thus proving that this protocol effectively hampers, from the point of view of cellulose arrangement, the degradation triggered by artificial ageing.

Finally, it is worth noting that the unilateral NMR device used for relaxation measurements permits the monitoring of the conservation status of cellulose in a completely noninvasive manner, thus possibly
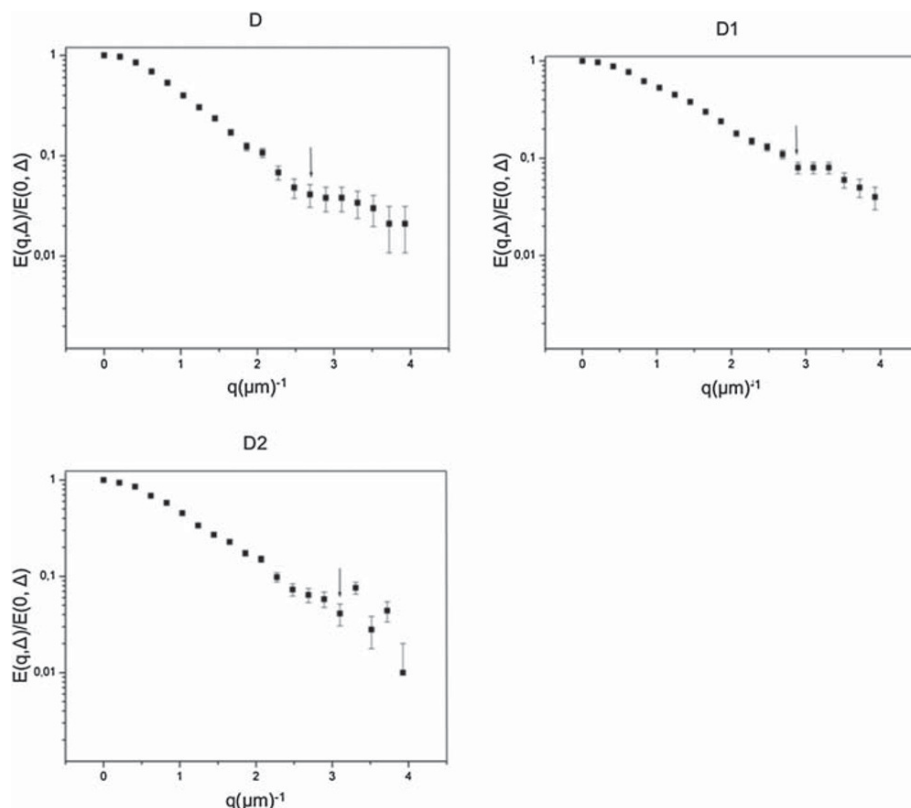
FIGURE 6 Nuclear magnetic resonance diffraction patterns of samples D, D1, and D2. Any arrow marks the first statistically significant dip

representing an effective tool for the analysis of cellulose-based artworks.

4 | CONCLUDING REMARKS

NMR relaxation and diffraction measurements of water trapped in the cellulose network of paper have been here used to indirectly investigate the changes in cellulose arrangement following an acidification bath and a consequent deacidification treatment by means of calcium hydroxide nanoparticles, as well as to relate such changes to the variation in DP following the ageing process.

As a result of the acidification treatment, the cellulose network gets opened, with a significant increase in pore size of ADs located in elementary fibrils at fibre surfaces. It is worth noting that this may also allow for the penetration of air pollutants from the external environment, inducing further degradation in cellulose-based artefacts. The effect of alkaline nanoparticles in preventing the acid-catalyzed degradation of cellulose is confirmed by NMR measurements: indeed, the neutralization of acids leads to a rearrangement of cellulose fibres into a more tightly packed conformation, resembling the cellulosic network of the reference system, even though, as expected, the DP of D sample is close to that of A sample.

The artificial ageing induces several modifications in the arrangement of cellulose network, mainly as a result of the increased mobility of cellulose chains and of the depolymerization occurring at random sites. After 1 week, the acidic sample displays a more compact arrangement of the fragmented molecules due to a further cellulose depolymerization, as confirmed by DP measurements. Correspondingly, the strong hampering of hydrothermal ageing due to the buffering action of nanoparticles results in spin-spin relaxation times of D1 and D2 similar to those of R1 and R2, respectively, confirming the beneficial effect of the applied deacidification treatment even upon ageing under strong conditions.

As a remark, NMR data presented in this work further corroborate the idea that calcium hydroxide nanoparticles are an effective tool to obstruct degradation of cellulose induced by acids and ageing under strong environmental conditions, also from the point of view of cellulose network arrangement. Relaxation data, in particular, were obtained using a noninvasive, portable instrumentation that can be considered a promising candidate for the monitoring of the conservation status of cellulose-based Cultural Heritage assets before and after a deacidification treatment.

ORCID

G. Poggi https://orcid.org/0000-0002-4158-0705
A. Parmentier https://orcid.org/0000-0002-9073-3288
S. Nourinaeini https://orcid.org/0000-0002-2656-4678

REFERENCES

[1] D. Fengel, G. Wegener, *Wood: Chemistry, Ultrastructure, Reactions*, Walter De Gruyter, Berlin and New York **1984**.

[2] K. Niskanen (Ed), *Paper Physics*, Fapet Oy, Helsinky (FIN) **1998**.

[3] H. Zhao, J. H. Kwak, Z. Conrad Zhang, H. M. Brown, B. W. Arey, J. E. Holladay, *Carbohydr. Polym.* **2007**, *68*, 235.

[4] D. Topgaard, O. Söderman, *Langmuir* **2001**, *17*, 2694.

[5] K. Nisizawa, *J. Ferment. Technol.* **1973**, *51*, 267.

[6] C. H. Stephens, P. M. Whitmore, H. R. Morris, M. E. Bier, *Biomacromolecules* **2008**, *9*, 1093.

[7] M. Müller, C. Riekel, R. Vuong, H. Chanzy, *Polymer (Guildf).* **2000**, *41*, 2627.

[8] K. C. Schuster, P. Aldred, M. Villa, M. Baron, R. Loidl, O. Biganska, S. Patlazhan, P. Navard, H. Rüf, E. Jericha, *Lenzinger Berichte* **2003**, *82*, 107.

[9] A. Conti, M. Palombo, A. Parmentier, G. Poggi, P. Baglioni, F. De Luca, *Cellul.* **2017**, *24*, 3479.

[10] A. Conti, G. Poggi, P. Baglioni, F. De Luca, F. De Luca, *Phys. Chem. Chem. Phys.* **2014**, *16*, 8409.

[11] L. Fan, M. M. Gharpuray, Y.-H. Lee, *Cellul. Hydrolys*, Springer Berlin Heidelberg, Berlin, Heidelberg **1987** 121.

[12] L. Lundgaard, W. Hansen, D. Linhjell, T. Painter, *Power Deliv. IEEE Trans.* **2004**, *19*, 230.

[13] N. Banait, W. Jencks, *J. Am. Chem. Soc.* **1991**, *113*, 7951.

[14] T. V. Dobrodskaya, P. A. Egoyants, V. K. Ikonnikov, N. D. Romashenkova, S. A. Sirotin, S. A. Dobrusina, N. I. Podgornaya, *Russ. J. Appl. Chem.* **2004**, *77*, 2017.

[15] M. Strlič, J. Kolar (Eds), *Ageing and Stabilization of Paper*, National And University Library, Ljubljana, Slovenia **2005**.

[16] J. Wouters, *Science (80-.).* **2008**, *322*, 1196.

[17] W. Yanjuan, F. Yanxiong, T. Wei, L. Chunying, *J. Cult. Herit.* **2013**, *14*, 16.

[18] M. Afsharpour, M. Hadadi, *J. Cult. Herit.* **2014**, *15*, 569.

[19] P. Baglioni, D. Chelazzi, *Nanoscience for the Conservation of Works of Art*, Royal Society Of Chemistry, Cambridge **2013**.

[20] P. Baglioni, D. Chelazzi, R. Giorgi, *Nanotechnologies in the Conservation of Cultural Heritage-A Compendium of Materials and Techniques*, Springer, Heidelberg New York London **2015**.

[21] J. W. Baty, C. L. Maitland, W. Minter, M. A. Hubbe, S. K. Jordan-Mowery, *BioResources* **2010**, *5*, 1955.

[22] S. Zervos, I. Alexopoulou, *Cellul.* **2015**, *22*, 2859.

[23] R. Giorgi, D. Chelazzi, P. Baglioni, *Langmuir* **2005**, *21*, 10743.

[24] R. Giorgi, D. Chelazzi, P. Baglioni, *Appl. Phys. A Mater. Sci. Process.* **2006**, *83*, 567.

[25] G. Poggi, N. Toccafondi, D. Chelazzi, P. Canton, R. Giorgi, P. Baglioni, *J. Colloid Interface Sci.* **2016**, *473*, 1.

[26] R. Giorgi, D. Chelazzi, E. Fratini, S. Langer, A. Niklasson, M. Rådemar, J.-E. Svensson, P. Baglioni, *J. Cult. Herit.* **2009**, *10*, 206.

[27] R. Giorgi, C. Bozzi, L. Dei, C. Gabbiani, B. W. Ninham, P. Baglioni, *Langmuir* **2005**, *21*, 8495.

[28] R. Giorgi, L. Dei, M. Ceccato, C. Schettino, P. Baglioni, *Langmuir* **2002**, *18*, 8198.

[29] G. Poggi, R. Giorgi, N. Toccafondi, V. Katzur, P. Baglioni, *Langmuir* **2010**, *26*, 19084.

[30] G. Poggi, P. Baglioni, R. Giorgi, *Restaurator* **2011**, *32*, 247.

[31] G. Poggi, N. Toccafondi, L. N. Melita, J. C. Knowles, L. Bozec, R. Giorgi, P. Baglioni, P. Baglioni, *Appl. Phys. A: Mater. Sci. Process.* **2014**, *114*, 685.

[32] G. Poggi, M. C. Sistach, E. Marin, J. F. Garcia, R. Giorgi, P. Baglioni, *J. Cult. Herit.* **2016**, *18*, 250.

[33] G. Poggi, R. Giorgi, A. Mirabile, H. Xing, P. Baglioni, *J. Cult. Herit.* **2017**, *26*, 44.

[34] S. Sequeira, C. Casanova, E. Cabrita, *J. Cult. Herit.* **2006**, *7*, 264.

[35] E. Stefanis, C. Panayiotou, *Restaurator* **2007**, *28*, 185.

[36] E. Stefanis, C. Panayiotou, *Restaurator* **2008**, *29*, 125.

[37] S. Bastone, D. F. Chillura Martino, V. Renda, M. L. Saladino, G. Poggi, E. Caponetti, *Colloids Surfaces A Physicochem. Eng. Asp.* **2017**, *513*, 241.

[38] K. L. Kato, R. E. Cameron, *Cellul.* **1999**, *6*, 23.

[39] S. Zervos, *Cellul.* **2007**, *14*, 375.

[40] UNI 8282, Cellulose in Dilute Solutions-Determination of Limiting Viscosity Number-Method in Cupri-Ethylene-Diamine (CED) Solution-Equivalent to the ISO Standard 5351/1, **1994**.

[41] A.-L. Dupont, G. Mortha, *J. Chromatogr. A* **2004**, *1026*, 129.

[42] P. Calvini, A. Gorassini, A. L. Merlani, *Cellul.* **2008**, *15*, 193.

[43] B. Blümich, J. Perlo, F. Casanova, *Prog. Nucl. Magn. Reson. Spectrosc.* **2008**, *52*, 197.

[44] C. Terenzi, C. Casieri, F. De Luca, *Appl. Clay Sci.* **2011**, *53*, 517.

[45] L. V. Y. -Q. Song, Y.-Q. Song, L. Venkataramanan, M. D. Hürlimann, M. Flaum, P. Frulla, C. Straley, *J. Magn. Reson.* **2002**, *154*, 261.

[46] C. Casieri, C. Terenzi, F. De Luca, *J. Appl. Phys.* **2009**, *105*, 034901.

[47] S. Peresada, A. Tonielli, R. Morici, C. S. Johnson, *Prog. Nucl. Magn. Reson. Spectrosc.* **1999**, *34*, 203.

[48] P. T. Callaghan, *Translational Dynamics and Magnetic Resonance: Principles of Pulsed Gradient Spin Echo NMR*, Oxford University Press, New York, NY **2011**.

[49] A. Lepore, S. Baccaro, C. Casieri, A. Cemmi, F. De Luca, *Chem. Phys. Lett.* **2012**, *531*, 206.

[50] A. M. Torres, R. J. Michniewicz, B. E. Chapman, G. A. R. Young, P. W. Kuchel, *Magn. Reson. Imaging* **1998**, *16*, 423.

[51] R. H. Atalla, in *Preserv. Pap. Text. Hist. Artist. Value II*, **1981**, pp. 169–176.

[52] S. Nourinaeini, G. Poggi, A. Parmentier, G. Rogati, P. Baglioni, F. De Luca, Submitt. to Cellul. **2019**. https://doi.org/10.1007/s10570-020-03298-0

[53] P. Calvini, *Cellul.* **2005**, *12*, 445.

[54] P. Bégin, S. Deschâtelets, D. Grattan, N. Gurnagul, J. Iraci, E. Kaminska, D. Woods, X. Zou, *Restaurator* **1999**, *20*, 1.

[55] E. Menart, G. De Bruin, M. Strlič, *Polym. Degrad. Stab.* **2011**, *96*, 2029.

[56] E. Menart, G. de Bruin, M. Strlič, *Cellul.* **2014**, *21*, 3701.

[57] A. Palme, H. Theliander, H. Brelid, *Carbohydr. Polym.* **2016**, *136*, 1281.

[58] C. P. Slichter, *Principles of Magnetic Resonance*, Springer Berlin Heidelberg, Berlin, Heidelberg **1990**.

[59] V. Bukovský, *Restaurator* **2000**, *21*, 55.

[60] P. Baglioni, D. Chelazzi, R. Giorgi, G. Poggi, in *Encycl. Surf. Colloid Sci*, Second ed. (Ed: P. Somasundaran), Taylor & Francis, New York **2012** 1.